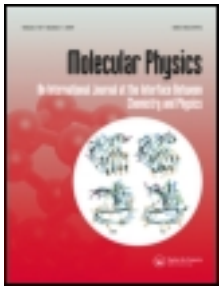

Molecular Physics: An International Journal at the Interface Between Chemistry and Physics
Publication details, including instructions for authors and subscription information:
http://www.tandfonline.com/loi/tmph20

External field control of spin-dependent rotational decoherence of ultracold polar molecules

Alexander Petrov [a b c], Constantinos Makrides [a d] & Svetlana Kotochigova [a]

[a] Department of Physics, Temple University, Philadelphia, PA, USA

[b] St. Petersburg Nuclear Physics Institute, Gatchina, Russia

[c] Division of Quantum Mechanics, Department of Physics, St. Petersburg State University, St. Petersburg, Russia

[d] Department of Physics and Astronomy, University of Toledo, Toledo, OH, USA

Published online: 14 Jun 2013.

To cite this article: Alexander Petrov, Constantinos Makrides & Svetlana Kotochigova (2013) External field control of spin-dependent rotational decoherence of ultracold polar molecules, Molecular Physics: An International Journal at the Interface Between Chemistry and Physics, 111:12-13, 1731-1737, DOI: 10.1080/00268976.2013.777812

To link to this article: http://dx.doi.org/10.1080/00268976.2013.777812

Molecular Physics, 2013
Vol. 111, Nos. 12–13, 1731–1737, http://dx.doi.org/10.1080/00268976.2013.777812

INVITED ARTICLE

External field control of spin-dependent rotational decoherence of ultracold polar molecules

Alexander Petrov[a,b,c], Constantinos Makrides[a,d] and Svetlana Kotochigova[a,*]

[a]*Department of Physics, Temple University, Philadelphia, PA, USA;* [b]*St. Petersburg Nuclear Physics Institute, Gatchina, Russia;* [c]*Division of Quantum Mechanics, Department of Physics, St. Petersburg State University, St. Petersburg, Russia;* [d]*Department of Physics and Astronomy, University of Toledo, Toledo, OH, USA*

(*Received 3 January 2013; final version received 13 February 2013*)

We determine trapping conditions for ultracold polar molecules, where pairs of internal states experience identical trapping potentials. Such conditions could ensure that detrimental effects of inevitable inhomogeneities across an ultracold sample are significantly reduced. In particular, we investigate the internal rovibronic and hyperfine quantum states of ultracold fermionic ground-state ^{40}K^{87}Rb polar molecules, when static magnetic, static electric and trapping laser fields are simultaneously applied. Understanding the effect of changing the relative orientation or polarisation of these three fields is of crucial importance for the creation of decoherence-free subspaces built from two or more rovibronic states. Moreover, we evaluate the induced dipole moment of the molecule in the presence of these fields, which will allow control of interactions between molecules in different sites of an optical lattice, and study the influence of the interaction anisotropy on the ability to entangle polar molecules.

Keywords: ultracold polar molecules; magic trapping conditions; polarisability; dipole moment

1. Introduction

The experimental realisation of a high-phase-space-density, quantum-degenerate gas of molecules, prepared in a single quantum state [1–4], opens up exciting prospects for the ultimate control of their internal and external degrees of freedom. In addition, significant progress has been made in loading and manipulating diatomic molecular species in periodic optical potentials [5–7]. Polar molecules are of particular interest in such experiments as they have permanent electric-dipole moments and therefore can interact via long-range tunable dipole–dipole interactions. Trapped in an optical lattice, these molecules can form new types of highly correlated quantum many-body states [8,9]. Moreover, it has been proposed [10] that they can be quantum bits of a scalable quantum computer. Finally, ultracold molecules are also promising systems to perform high-precision measurements of a possible time variation of fundamental physical constants. In parallel, there is a growing interest in orienting (non-degenerate) polar molecules using intense pulsed AC fields sometimes combined with an external static electric field [11–13]. The feasibility of orienting rotationally cold polar molecules in an external field has been demonstrated [14,15].

Molecules have complex vibrational, rotational and hyperfine internal structure with many internal degrees of freedom [16,17]. As was shown in recent experiments [5,18], coherent control over internal quantum states of molecules plays a key role in manipulation of molecules with a long coherence time. An important property for controlling a molecule with light fields is its complex molecular dynamic polarisability $\alpha(h\nu, \vec{\epsilon})$ at radiation frequency ν and polarisation $\vec{\epsilon}$ (h is Planck's constant). Multiplied with the laser intensity, its real part determines the strength of a lattice potential. As different internal states have different polarisability, their lattice depths or Stark shifts differ.

A second important property of polar molecules is its permanent dipole moment. Their rotational levels can be shifted and mixed with one another by applying an external electric field. In the presence of both, a static external electric field and laser fields, the ground state has an anisotropic polarisability [2]. The anisotropy of the dynamic polarisability of these levels manifests itself as a dependence on the relative orientation of the polarisation of the trapping laser and the DC electric field. Finally, alkali-metal polar molecules have a non-zero nuclear electric-quadrupole and nuclear-magnetic moments of the constituent atoms. Then, by applying a magnetic field, quadrupole and Zeeman interactions further mix states. The combined action of these three fields can be a powerful tool with which to manipulate and control ultracold molecules trapped in an optical potential.

For many applications of ultracold polar molecules, it is advantageous or even required that two or more molecular rotational-hyperfine states have the same spatial trapping

*Corresponding author. Email: skotoch@temple.edu

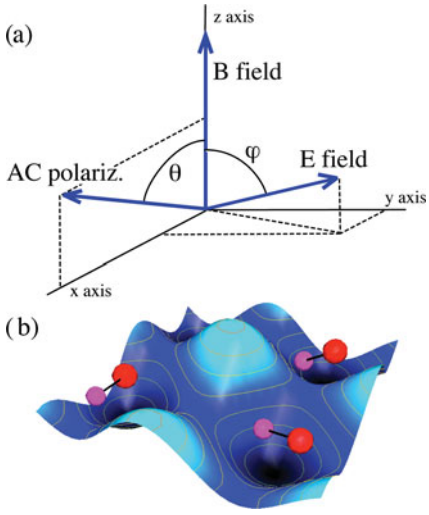

Figure 1. (Colour online) Panel (a) shows the orientations of the static electric and magnetic fields as well as the AC polarisation of the optical trapping laser. Without loss of generality, we assume that the magnetic field, $\vec{B}$, is directed along the z-axis, while the polarisation $\vec{\epsilon}$ of the laser lies in the x–z plane. The electric field $\vec{E}$ can be in any direction. Only two of the three angles that uniquely specify the relative orientations are indicated. Panel (b) shows a cartoon of polar molecules held in an optical lattice potential with polarisation $\vec{\epsilon}$.

potential. This is a so-called 'magic' condition. In atomic gases magic conditions occur for specific off-resonant laser frequencies [19–21]. In molecular systems, such frequencies exist when light resonant or nearly resonant with molecular transitions is used [22]. Unwanted spontaneous emission can then lead to dephasing. Recent experimental and theoretical studies [18,23] of ground-state polar molecules demonstrated that 'magic' conditions can exist for off-resonant laser frequencies as long as the angle between the laser polarisation and either an external magnetic field or an external electric field is carefully controlled. In fact, Ref. [18] showed in measurements of the AC polarisability and the coherence time for microwave transitions between rotational states that there exists a 'magic' angle between the orientation of the polarisation of the trapping light and a magnetic field. In this experiment, no electric field was applied.

Here we extend the ideas of Refs. [16–18,23] and perform a theoretical study of the internal rovibronic and hyperfine quantum states of the KRb molecules when simultaneously static magnetic and electric fields as well as non-resonant trapping lasers are applied. A schematic diagram is shown in Figure 1. The purpose of the study is to develop a quantitative model for energy levels, polarisibility and dipole moments for an efficient quantum coherent control of coupled rotational states. Our research is closely linked to ongoing experiments with ultracold KRb molecules [5,6,18]. Understanding the effect of changing the relative orientation or polarisation of these three fields is of crucial importance for the creation of decoherence-free subspaces built from two or more rovibronic and hyperfine states.

We also evaluate the imaginary part of the polarisability, due to spontaneous emission from excited electronic states. Here, the imaginary part is calculated assuming that excited vibrational levels have a linewidth evaluated by either using the linewidth of atomic K or Rb or using an optical-potential approach [24].

This paper is set up as follows. In Section 2, we construct the Hamiltonian of the rotating KRb molecule in the presence of the three external fields. We then present results of our calculation of the AC polarisability in Section 3. The dipole moment is calculated as a function of electric field in Section 4. We finish with a discussion of the imaginary part of the polarisability due to spontaneous emission of electronic excited states in Section 5.

2. Molecular Hamiltonian

We focus on rotational states of the lowest vibrational level of the singlet $X^1\Sigma^+$ ground-state potential of $^{40}K^{87}Rb$ in the presence of a magnetic and electric field as well as an AC trapping laser field. We denote the rotational states by the angular momentum quantum number N and its projection m_N onto the external magnetic field direction. Both K and Rb have non-zero nuclear spin, which aligns along the magnetic field, through the Zeeman interaction. Nuclear quadrupole interactions mix these nuclear hyperfine states with the rotation of the molecule. The relative directions of the fields are defined in Figure 1. Throughout, angular momentum and tensor algebra is based on Ref. [25].

In practice, we have determined the molecular polarisability and dipole moment starting from the molecular basis functions or channels:

$$|N, m_N, m_a, m_b\rangle \equiv \phi_{v=0}(r)\,|X^1\Sigma^+\rangle\, Y_{Nm_N}(\alpha\beta)\,|i_a m_a, i_b m_b\rangle, \quad (1)$$

where $\phi_{v=0}(r)$ is the $v = 0$ radial vibrational wavefunction for interatomic separation r, which for the small N studied here is to good approximation independent of N, and $|X^1\Sigma^+\rangle$ is the electron wavefunction with projections defined along the internuclear axis. The spherical harmonic $Y_{Nm_N}(\alpha\beta)$ describes the rotational wavefunction of our Σ molecule. The angles α and β and projection m_N are defined with respect to the magnetic field direction. The nuclear spins $\vec{i}_a$ and $\vec{i}_b$ for atoms a and b have values i_a and i_b and projections m_a and m_b onto the magnetic field. For $^{40}K^{87}Rb$ there are 144 channels $|N, m_N, m_a, m_b\rangle$ with $N = 0$ and 1. The degeneracy of states with projections m_N for the same N is lifted by the interaction between the nuclear quadrupole moment and the rotation of the molecule [5,18]. Here we focus on hyperfine states whose dominant

nuclear spin character is $m_a = -4$, $m_b = 1/2$ for ^{40}K and ^{87}Rb, respectively. These states were selected for the experimental measurement of the dynamic polarisability in the ground-state KRb molecule [18].

The effective Hamiltonian for the $v = 0$ rotational-hyperfine levels is given by

$$H = H_{\rm rot} + H_Z + H_E + H_Q + H_{\rm pol}\,, \tag{2}$$

and

$$H_{\rm rot} = B_v \vec{N}^2 \tag{3}$$

$$H_Z = -\sum_{k=a,b} \mu_k \vec{\imath}_k \cdot \vec{B} \tag{4}$$

$$H_E = -\vec{d} \cdot \vec{E} \tag{5}$$

$$H_Q = \sum_{k=a,b} Q_k C_2(\alpha\beta) \cdot T_2(\vec{\imath}_k, \vec{\imath}_k) \tag{6}$$

$$H_{\rm pol} = -\left(\alpha_\parallel \mathcal{O}_\parallel + \alpha_\perp \mathcal{O}_\perp\right) I\,, \tag{7}$$

where $H_{\rm rot}$ is the rotational Hamiltonian with vibrationally averaged rotational constant $B_v = \int_0^\infty dr \phi_v(r) \hbar^2/(2\mu r^2) \phi_v(r)$, where μ is the reduced mass and $\hbar = h/2\pi$. The matrix operator of $H_{\rm rot}$ is diagonal with our basis functions. For the KRb dimer, the energy spacing Δ between the vibrational levels $v = 0$ and $v = 1$ is of the order of $\Delta/h = 1500$ GHz, while $B_v/h = 1.1139$ GHz for $v = 0$ [1].

The next term in the Hamiltonian is the nuclear Zeeman interaction H_Z for each atom, where μ_k is the nuclear magneton of atom k [26] and $\vec{B}$ is the magnetic field and only affects the nuclear spins. This contribution is followed by the electric-dipole interaction H_E, which describes the effect of a static electric field $\vec{E}$ and contains the vibrationally averaged molecular dipole moment operator $\vec{d}$. Matrix elements of H_E follow the realisation that H_E can equivalently be written as $-d_0 \sum_{q=-1}^{1} (-1)^q C_{1q}(\alpha\beta) E_q$, where $d_0 = \int_0^\infty dr\, \phi_{v=0}(r) \mathcal{D}(r) \phi_{v=0}(r)$ and $\mathcal{D}(r)$ is the r-dependent permanent electric-dipole moment of the $X^1\Sigma^+$ potential. Moreover, E_q are the rank-1 spherical components of $\vec{E}$ and $C_{lm}(\alpha\beta) = \sqrt{4\pi/(2l+1)} Y_{lm}(\alpha\beta)$ is a spherical harmonic of rank l. It follows that matrix elements are non-zero when $N + 1 + N'$ is even. We use $d_{v=0} = 0.223 e a_0$ for KRb, where e is the electron charge and $a_0 = 0.05292$ nm is the Bohr radius. The value is consistent with the result of Ref. [1].

Equation (2) also includes the nuclear quadrupole interaction H_Q for each atom. It has coupling constants Q_k and couples the nuclear spin to rotational states. Here, $T_{2m}(\vec{\imath}_k, \vec{\imath}_k)$ is a rank-2 tensor constructed from spin $\vec{\imath}_k$. For KRb the two quadrupole parameters Q_k were first determined in Ref. [5] based on measurements of transition energies between sublevels of the $N = 0$ and $N = 1$ states. We use the more recent values $Q_K/h = 0.452$ MHz and $Q_{Rb}/h = -1.308$ MHz from [18].

Finally, we must include a term that describes the 'reduced' AC Stark shift $H_{\rm pol}$ with strengths $\alpha_\parallel$ and $\alpha_\perp$, rank-2 tensor operators $\mathcal{O}_\parallel$ and $\mathcal{O}_\perp$, and laser intensity I [23]. This Stark shift is 'reduced' in the sense that it is the Stark shift of the molecule when the other terms in our Hamiltonian are ignored and the 'reduced' polarisabilities $\alpha_\parallel$ and $\alpha_\perp$ only depend on the laser frequency. In fact, these two polarisabilities can be expressed in terms of a sum over rovibrational states of all excited $^1\Sigma^+$ and $^1\Pi$ electronic potentials, respectively. The operators $\mathcal{O}_\parallel$ and $\mathcal{O}_\perp$ capture all dependence on light polarisation and rotational angular momentum $\vec{N}$. For a 1063 nm laser $\alpha_\parallel/h = 10.0 \times 10^{-5}$ MHz/(W/cm^2) and $\alpha_\perp/h = 3.3 \times 10^{-5}$ MHz/(W/cm^2) measured in Ref. [18].

We find eigenenergies of this Hamiltonian by diagonalisation, including rotational levels $N \leq 20$, and analyse its eigenfunctions to connect to states that have been observed experimentally. Eigenstates can be identified by the channel state with the largest contribution, although for field strengths and laser intensities accessible in ultracold molecular experiments we expect that the eigenstates can be severely mixed. The polarisability of eigenstate j with energy $\mathcal{E}_j(I, E)$ is defined as the derivative $\alpha_j = -d\mathcal{E}_j/dI$, while the dipole moment of state j is $\vec{d}_j = -d\mathcal{E}_j/d\vec{E}$. In this paper, these two quantities are studied as a function of angles θ and φ, defined in Figure 1(a), magnetic field strength B, electric field strength E and intensity I of the trapping laser field.

3. Real part of polarisability

In this section, we present results for the dynamic polarisability of the $N = 0$ and $N = 1$ rotational levels of the $v = 0$ vibrational level of the ground $X^1\Sigma^+$ state of ^{40}K^{87}Rb. The molecules are placed in an optical dipole trap created from a focussed laser with a wavelength of 1063 nm. An external magnetic field of $B = 545.9$ G and a static electric field are also present. The values of the fields and laser intensities are based on recent measurements with ultracold KRb molecules [18].

Figure 2 shows the polarisability as a function of θ and φ based on the Hamiltonian in Equation (2) and the geometry defined in Figure 1(a) for four rotational-hyperfine states. The laser intensity $I = 2.35$ kW/cm^2 and the electric field strength $E = 1$ kV/cm. We focus on the four states that have a predominant $|N, m_N, m_a, m_b\rangle = |0, 0, -4, 1/2\rangle$, $|1, 0, -4, 1/2\rangle$ and $|1, \pm 1, -4, 1/2\rangle$ character as they are of experimental interest. We observe that the polarisabilities of $N = 1$ states change noticeably when going from small to large values of the angles, while that for $|0, 0, -4, 1/2\rangle$ does not change for any angle. Figure 2 shows that the polarisabilities of hyperfine levels coincide for many values

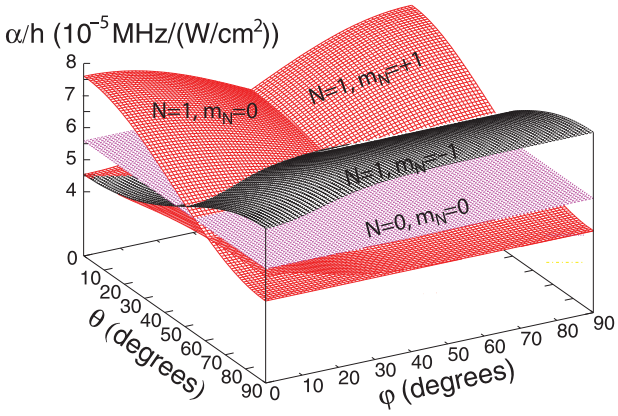

Figure 2. Polarisability of four rotational-hyperfine states of the $v = 0$ vibrational level of the $X^1\Sigma^+$ potential of KRb as a function of angle θ between the polarisation of the dipole-trap laser and magnetic field, and as a function of angle φ between the static electric and magnetic fields. The electric field lies in the y–z plane as defined in Figure 1. The magnetic field strength $B = 545.9$ G, the electric field strength $E = 1$ kV/cm and the laser at 1063 nm has an intensity of $I = 2.35$ W/cm^2. The four surfaces are labelled by the rotational levels $|N, m_N\rangle = |0, 0\rangle$, $|1, 0\rangle$, $|1, -1\rangle$ and $|1, +1\rangle$, respectively. Their nuclear spin wavefunction is $m_a = -4$ and $m_b = 1/2$ for potassium and rubidium, respectively.

of θ and ϕ. Crossings of polarisabilities correspond to the so-called 'magic' angles θ and φ, where the differential Stark shift for two or more states is zero. In fact, Figure 3 shows that the magic angles between the states $|0, 0, -4, 1/2\rangle$ and $|1, 0, -4, 1/2\rangle$ form a nearly-circular, elliptical curve that starts at $\theta = 57^\circ$ and $\varphi = 0^\circ$.

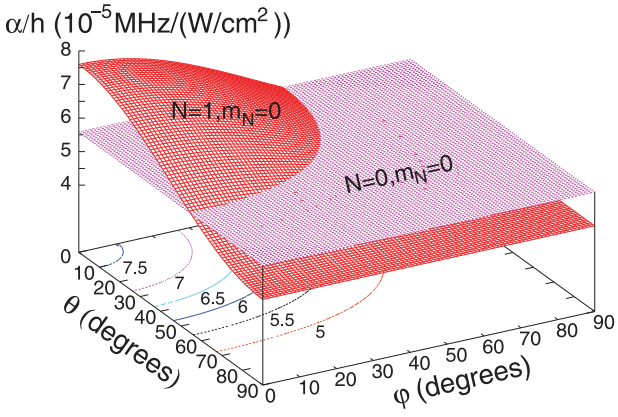

Figure 3. Polarisability of two $m_N = 0$ rotational-hyperfine states of the $v = 0$ vibrational level of the $X^1\Sigma^+$ potential of KRb as a function of angles θ and φ. Six contours of constant polarisability of the $|N = 1, m_N = 0\rangle$ state are plotted as well. The polarisability of the $|N = 0, m_N = 0\rangle$ state is independent of the two angles. The contour marked by 5.5 approximately corresponds to 'magic' conditions for the two $m_N = 0$ rotational-hyperfine states. Parameters and remaining orientation are as for Figure 2.

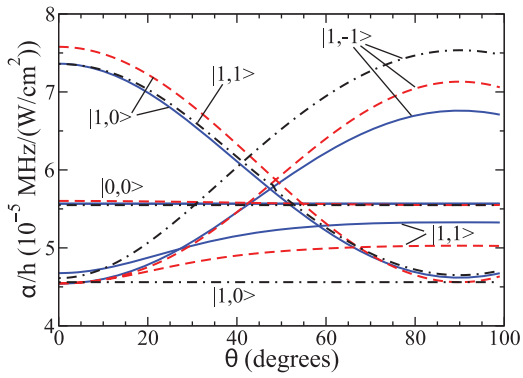

Figure 4. Polarisability of four rotational-hyperfine states of the $v = 0$ vibrational level of the $X^1\Sigma^+$ potential of KRb as a function of angle θ between the polarisations of the dipole-trap laser for three configurations of the electric field. The solid blue lines are for zero electric field. They were previously published in Ref. [18]. The red dashed lines are for an electric field with a strength of 1 kV/cm oriented parallel to the magnetic field ($\varphi = 0^o$), while the dot–dashed black lines are for $E = 1$ kV/cm oriented in the y–z plane but perpendicular to the magnetic field ($\varphi = 90^o$). The remaining parameters and nuclear hyperfine states are as for Figure 2 and note that the x-axis extends to 100°.

Figures 4 and 5 show cuts through the surfaces depicted in Figures 2 and 3 in order to facilitate a quantitative comparison. Figure 4 shows the polarisability for four rotational-hyperfine states as a function of θ without an applied electric field as well as for $E = 1$ kV/cm oriented either parallel ($\varphi = 0^o$) and perpendicular ($\varphi = 90^o$) to the magnetic field. The curves for zero electric field and that for $E = 1$ kV/cm with $\varphi = 0^o$ are similar in shape and predict 'magic' conditions between $\theta = 50^o$ and 60^o. The polarisability for the $|1, 0, -4, 1/2\rangle$ state decreases by as much as a factor of 2 for increasing θ. On the other hand, for $E = 1$ kV/cm and $\varphi = 90^o$ the polarisabilities of $|0, 0, -4, 1/2\rangle$

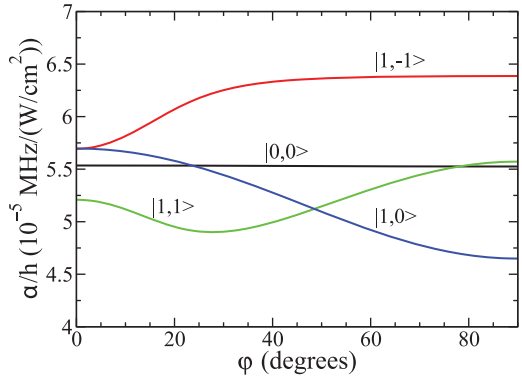

Figure 5. Polarisability of four rotational-hyperfine states of the lowest vibrational level of the $X^1\Sigma^+$ potential of KRb as a function of angle φ between the electric field and the magnetic field and $\theta = 51^\circ$. For this value of θ the 'magic' angle φ is 23°. All other parameters are the same as for Figure 2.

and $|1, 0, -4, 1/2\rangle$ do not cross. In fact, the polarisability of the $|1, 0, -4, 1/2\rangle$ state is nearly independent of angle θ, while that for the $|1, 1, -4, 1/2\rangle$ state now decreases by a factor of 2 for increasing θ.

Figure 5 shows the polarisability for the same four states as a function of φ for one value of θ and $E = 1$ kV/cm. For this value of θ, the magic condition between the states $|0, 0, -4, 1/2\rangle$ and $|1, 0, -4, 1/2\rangle$ occurs at the relatively small angle $\varphi = 23^{\circ}$. On the other hand, the polarisability of the $|1, -1, -4, 1/2\rangle$ state does not coincide with that of the $|0, 0, -4, 1/2\rangle$ state at any angle φ.

Our analyses show that for a trapping laser light at 1063 nm and external electric field strengths of 1 kV/cm only a few low-lying rotational states are mixed. The near-infrared laser frequency is detuned away from resonances with rovibrational levels of the electronically excited potentials. As a result, corrections to the polarisability from the level shifts due to the static electric and magnetic fields are significantly suppressed.

4. Induced dipole moment

Figure 6 shows the induced dipole moment of four rotational-hyperfine levels along the electric field direction as a function of the electric field strength E. We assume an angle $\theta = 51^{\circ}$ between the magnetic field and the laser polarisation and angle $\varphi = 23^{\circ}$ between the electric and magnetic fields, to ensure that the $|N, m_N\rangle = |0, 0\rangle$ and $|1, 0\rangle$ states have the same polarisability at $E = 1$ kV/cm. The nuclear spin state is $m_a = -4$ and $m_b = 1/2$. For $E <$ 7 kV/cm the dipole moment of the $|1, 0\rangle$ state decreases with E and is negative. On the other hand, the dipole moments of the $|0, 0\rangle$ and $|1, \pm 1\rangle$ states always increase with E and are positive. For $E \gg 10$ kV/cm, the induced dipole moments of all four rotational-hyperfine levels converge to $d_0 = 0.223ea_0$. From results not shown here, we find that

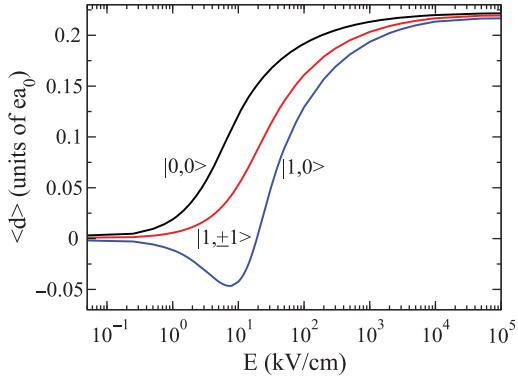

Figure 6. (Colour online) The induced dipole moment of the lowest rotational levels of the $v = 0$ vibrational level of the $X^1\Sigma^+$ potential of $^{40}K^{87}Rb$ as a function of external electric field strength E. The angles θ and φ are 51° and 23°, respectively. The laser intensity, remaining orientation and magnetic field strength are the same as for Figure 2.

the induced dipole moment is aligned along the direction of the electric field, $\vec{d}_j \propto \vec{E}$, and that the magic conditions are nearly independent of the electric field strength. Both observations follow from the fact that $m_a = -4$ and $m_b = 1/2$ are approximately good quantum numbers and that, for fields shown in Figure 6, H_E is much larger than H_Z and H_Q. The coupling between rotational and nuclear spin states is weak. Then, for small electric field strengths, the four $\vec{d}_j$ follow the second-order perturbation theory expressions

$$\begin{aligned}
\vec{d}_{N,m_N=0,0} &= 2\frac{d_0^2|\langle 0,0|C_{10}|1,0\rangle|^2}{2B_v}\vec{E};\\
\vec{d}_{1,0} &= 2\left[-\frac{d_0^2|\langle 0,0|C_{10}|1,0\rangle|^2}{2B_v}+\frac{d_0^2|\langle 2,0|C_{10}|1,0\rangle|^2}{4B_v}\right]\vec{E};\\
\vec{d}_{1,\pm1} &= 2\frac{d_0^2|\langle 2,\pm1|C_{10}|1,\pm1\rangle|^2}{2B_v}\vec{E}\,.
\end{aligned} \tag{8}$$

The induced dipole moments of the $|N, m_N\rangle = |0, 0\rangle$ and $|1, \pm 1\rangle$ states have a single contribution from transitions to states with $N' = N + 1$ with larger rotational energies. This leads to a positive dipole moment. For the dipole moment of the $|N, m_N\rangle = |1, 0\rangle$ state, contributions from the state with both smaller and larger rotational energies appear. In this case, their combined effect leads to a negative dipole moment.

5. Imaginary part of the polarisability

The Hamiltonian described in Section 2 does not describe losses due to spontaneous emission of rovibrational levels of electronically excited states. These losses appear as an imaginary contribution to the polarisability. We can understand this by realising that at a specific laser intensity magnetic field and electric field the complex-valued polarisability of state i can also be defined as

$$\begin{aligned}
\alpha(h\nu,\vec{\epsilon}) = \frac{1}{\epsilon_0 c}\sum_f \frac{(E_f - ih\gamma_f/2 - E_i)}{(E_f - ih\gamma_f/2 - E_i)^2 - (h\nu)^2}\\
\times|\langle f|\vec{d}_{\rm tr}\cdot\vec{\epsilon}|i\rangle|^2\,,
\end{aligned} \tag{9}$$

where c is the speed of light, ϵ_0 is the electric constant, and the kets $|i\rangle$ and $|f\rangle$ denote the initial and intermediate rotational-and-hyperfine-resolved vibrational wavefunctions of the $|X^1\Sigma^+\rangle$ potential and excited electronic states. Their energies are E_i and E_f, respectively. The matrix elements $\langle f|\vec{d}_{\rm tr}|i\rangle$ are vibrationally averaged electronic transition dipole moments and $\vec{\epsilon}$ is the polarisation of the laser. The sum over f excludes the initial state but includes transitions to the rovibrational levels within the $X^1\Sigma^+$ potential as well as to the rovibrational levels of excited potentials. Contributions from scattering states or the continuum of any state must also be included. For alkali-metal dimers, this sum, however, can be limited to transitions to electronic excited potentials that dissociate to either a singly excited

K or a singly excited Rb atom as only those have significant electronic dipole moments to the $X^1\Sigma^+$ state. Moreover, as we focus on the KRb polarisability for an infrared laser with a 1063 nm wavelength, their contribution is further reduced by the energy denominator in Equation (9). Finally, the natural linewidths γ_f of excited rovibrational levels describe the spontaneous emission that lead to loss of molecules by emission of a spontaneous photon.

As currently only a single measurement of the imaginary part of the polarisability [27] is available to characterise the imaginary part of the two 'reduced' polarisabilities of $H_{\rm pol}$ in Equation (2), we can only compare this $\vec{E} = \vec{0}$ measurement to *ab initio* theoretical estimates based on Equation (9). To calculate the theoretical dynamic polarisability, we use the most accurate ground-state potentials available from Ref. [28]. Excited potentials are constructed from RKR data [29,30] and as well as from our *ab initio* calculations [31] using long-range dispersion coefficients from Ref. [32]. We employ transition dipole moments from our previous electronic structure calculations of KRb [33,34].

We evaluate the linewidths of excited rovibrational states using two different methods. In the first method, the imaginary part of the polarisability is calculated assuming that the linewidth of rovibrational levels of the $X^1\Sigma^+$ potential is zero and that rovibrational levels of the lowest excited electronic potentials that dissociate to either a singly excited K atom or a singly excited Rb atom have a natural linewidth equal to the atomic linewidth of potassium. The small, less than 1% difference in linewidth of K and Rb does not modify our results significantly.

For our second method, the molecular linewidth of vibrational levels of potentials that dissociate to either a singly excited K or a singly excited Rb atom is calculated assuming an 'optical potential' $i\Gamma(r)/2$ [24], where $\Gamma(r)$ is proportional to $\omega(r)^3 d(r)^2$, the frequency $\omega(r)$ is the transition frequency between the two potentials at each r, and $d(r)$ is the r-dependent transition dipole moment. This is essentially a stationary-phase approximation. The number of electronic potentials included is the same as for the first method.

Figure 7 shows the calculated imaginary part of the polarisability as a function of angle θ for the two means of including the effect of spontaneous emission. The value of the imaginary part is always negative and is seven orders of magnitude smaller than the real part. Even though this imaginary part is small, it will affect precision measurements with ultracold KRb molecules. The figure also shows that the absolute value of Im α is larger for the second method of modelling spontaneous emission. This is because the molecular transition dipole moments from the excited state to the ground state at the equilibrium separation R_e is larger than the atomic dipole moment. The measured Im $\alpha = -2.1(2) \times 10^{-12}$ MHz/(W/cm^2) for the $|N, m_N\rangle = |0, 0\rangle$ state and $\theta = 45^\circ$ [27] is in better agreement with the model that uses the atomic linewidth.

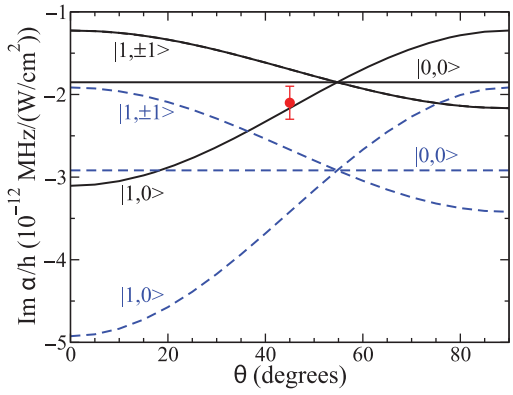

Figure 7. (Colour online) Imaginary part of polarisability of the $N = 0$ and 1 rotational levels of the $v = 0$ vibrational level of the $X^1\Sigma^+$ potential of KRb as a function of angle θ between the polarisation of the dipole-trap laser at 1063 nm and bias magnetic field with strength $B = 545.9$ G. The static electric field strength is zero. The laser has an intensity of $I = 2.35$ W/cm^2. Results for two different ways of determining the imaginary polarisability are shown. The solid lines correspond to Im α, when the linewidth of excited rovibrational levels equals the atomic linewidth of K; the dashed lines are obtained using excited-state linewidths obtained with an 'optical potential' approach. The only experimental measurement of the imaginary polarisability for the $|N, m_N\rangle = |0, 0\rangle$ state and $\theta = 45^\circ$ [27] is shown by the red marker with an error bar.

6. Summary

We performed a theoretical study of the internal rovibronic and hyperfine quantum states of the KRb molecules when simultaneously static magnetic and electric fields as well as trapping lasers are applied. The combined action of these fields can be used for an efficient quantum control of ultracold polar molecules in optical potentials. We extended the ideas of mixing rotational levels in Refs. [18,23] to include all three fields as in typical ultracold experiments. In particular, we searched for 'magic' angles between the external DC electric, magnetic and AC trapping fields, where the AC Stark shift of pairs of rotational states is the same. Moreover, we evaluated the induced dipole moment of the internal rovibronic and hyperfine quantum states as a function of external electric field. With this precise value of the dipole moment, one can investigate how interactions between molecules in the different optical lattice sites depend on the relative orientation of the applied fields. Our theoretical research efforts are closely linked to ongoing experiments with ultracold KRb molecules.

Acknowledgements

We acknowledge funding from the Army Research Office MURI on High-Resolution Quantum Control of Chemical Reactions. This research was also supported in part by the National Science Foundation under Grants No. PHY11-25915 and PHY10-05453.

References

[1] K.-K. Ni, S. Ospelkaus, M.H.G. de Miranda, A. Pe'er, B. Neyenhuis, J.J. Zirbel, S. Kotochigova, P.S. Julienne, D.S. Jin, and J. Ye, Science **322**, 231 (2008).

[2] S. Ospelkaus, K.-K. Ni, M.H.G. de Miranda, B. Neyenhuis, D. Wang, S. Kotochigova, P.S. Julienne, D.S. Jin, and J. Ye, Faraday Discuss. **142**, 361 (2009).

[3] J. G. Danz, E. Haller, M. Gustavsson, N. Bouloufa, O. Dulieu, H. Ritsch, and H.-C. Nägerl, Faraday Discuss. **142**, 283 (2009).

[4] J.G. Danz, M.J. Mark, E. Haller, M. Gustavsson, R. Hart, J. Aldegunde, J.M. Hudson, and H.-C. Naägerl, Nature Phys. **6**, 265 (2010).

[5] S. Ospelkaus, K.-K. Ni, G. Quéméner, B. Neyenhuis, M.H.G. de Miranda, J.L. Bohn, J. Ye, and D. S. Jin, Phys. Rev. Lett. **104**, 030402 (2010).

[6] M.H.G. de Miranda, A. Chotia, B. Neyenhuis, D. Wang, G. Quéméner, S. Ospelkaus, J.L. Bohn, J. Ye, and D.S. Jin, Nature Phys. **7**, 502 (2011).

[7] J.G. Danz, E. Haller, M. Gustavsson, M.J. Mark, R. Hart, N. Bouloufa, O. Dulieu, H. Ritsch, and H.-C. Nägerl, Science **321**, 1062 (2008).

[8] M. Baranov, Phys. Rep. **464**, 71 (2008).

[9] T. Lahaye, C. Menotti, L. Santos, M. Lewenstein, and T. Pfau, Rep. Prog. Phys. **72**, 126401 (2009).

[10] D. DeMille, Phys. Rev. Lett. **88**, 067901 (2002).

[11] B. Friedrich and D. Herschbach, Nature **353**, 412 (1991).

[12] J.M. Rost, J.C. Griffin, B. Friedrich, and D. Herschbach, Phys. Rev. Lett. **68**, 1299 (1992).

[13] B. Friedrich and D. Herschbach, J. Chem. Phys. **99**, 15686 (1995).

[14] H. Sakai, S. Minemoto, H. Nanjo, H. Tanji, and T. Suzuki, Phys. Rev. Lett. **90**, 083001 (2003).

[15] J. H. Nielsen, H. Stapelfeldt, J. Küpper, B. Friedrich, J.J. Omiste, and R. González-Férez, Phys. Rev. Lett. **108**, 193001 (2012).

[16] J. Aldegunde, B.A. Rivington, P.S. Zuchowski, and J.M. Hudson, Phys. Rev. A **78**, 033434 (2008).

[17] J. Aldegunde, H. Ran, and J.M. Hudson, Phys. Rev. A **80**, 043410 (2009).

[18] B. Neyenhuis, B. Yan, S.A. Moses, J.P. Covey, A. Chotia, A. Petrov, S. Kotochigova, J. Ye, and D.S. Jin, Phys. Rev. Lett. **109**, 230403 (2012).

[19] J. Ye, H.J. Kimble, and H. Katori, Science **320**, 1734 (2008).

[20] N. Lundblad, M. Schlosser, and J.V. Porto, Phys. Rev. A **81**, 031611(R) (2010).

[21] A. Derevianko and H. Katori, Rev. Mod. Phys. **83**, 331 (2011).

[22] T. Zelevinsky, S. Kotochigova, and J. Ye, Phys. Rev. Lett. **100**, 043201 (2008).

[23] S. Kotochigova and D. DeMille, Phys. Rev. A **82**, 063421 (2010).

[24] B. Zygelman and A. Dalgarno, Phys. Rev. A **38**, 1877 (1988).

[25] D.M. Brink and G.R. Satchler, *Angular Momentum*, 3rd ed. (Clarendon Press, Oxford, 1993).

[26] E. Arimondo, M. Inguscio, and P. Violoni, Rev. Mod. Phys. **49**, 31 (1977).

[27] A. Chotia, B. Neyenhuis, S.A. Moses, B. Yan, J.P. Covey, M. Foss-Feig, A.M. Rey, and J. Ye, Phys. Rev. Lett. **108**, 080405 (2012).

[28] A. Pashov, O. Docenko, M. Tamanis, R. Ferber, H. Knöckel, and E. Tiemann, Phys. Rev. A **76**, 022511 (2007).

[29] S. Kasahara, C. Fujiwara, N. Okada, and H. Katô, J. Chem. Phys. **111**, 8857 (1999).

[30] C. Amiot, J. Mol. Spect. **203**, 126 (2000).

[31] S. Kotochigova, E. Tiesinga, and P.S. Julienne, New J. Phys. **11**, 055043 (2009).

[32] B. Bussery, Y. Achkar, and M. Aubert-Freçon, Chem. Phys. **116**, 319 (1987).

[33] S. Kotochigova, P.S. Julienne, and E. Tiesinga, Phys. Rev. A **68**, 022501 (2003).

[34] S. Kotochigova, E. Tiesinga, and P.S. Julienne, Eur. Phys. J. D **31**, 189 (2004).